

Cognitive Modes Detectable with Task-Based fMRI:
Review and Pattern-Based Anatomy

Linda Chen^{1,2}

&

Todd S. Woodward^{1,2}

¹BC Mental Health and Addictions Research Institute, Provincial Health Services Authority,
Vancouver, BC, Canada

²Department of Psychiatry, University of British Columbia, Vancouver, BC, Canada

*Please address all correspondence to: Todd S. Woodward, Ph. D., Room A3-A117, BC Mental Health & Addictions Research Institute – Translational Research Building, 3rd Floor, 938 W. 28th Avenue, Vancouver, British Columbia, Canada, V5Z 4H4, fax: 604-875- 3871, phone: 604-875-2000 x 4724, e-mail: Todd.S.Woodward@gmail.com.

Table of Contents

| | |
|--|----|
| Introduction on fMRI | 3 |
| The 11 Cognitive Modes | 4 |
| Response (One-Handed 1RESP & Two-Handed 2RESP) | 4 |
| Maintaining Internal Attention (MAIN) | 7 |
| Multiple Demand (MD) | 9 |
| Initiation (INIT) | 11 |
| Auditory Perception (AUD) | 13 |
| Re-Evaluation (RE-EV) | 14 |
| Language (LAN) | 16 |
| Auditory Attention for Response (AAR) | 18 |
| Focus on Visual Features (FoVF) | 20 |
| Default Mode A (DMA) | 22 |
| Default Mode B (DMB) | 24 |
| References | 26 |

Introduction on fMRI

Functional magnetic resonance imaging (fMRI) is a non-invasive neuroimaging technique for assessing brain activity primarily utilized to map the spatiotemporal distribution and patterns of neural activity under varying cognitive conditions.

fMRI technology leverages the blood oxygen level-dependent (BOLD) contrast, reflecting the interplay between neural activity, oxygen consumption, and blood flow (Buchbinder, 2016). When neurons in a particular area of the brain are active, they consume more oxygen, which is delivered by an increase in local blood flow (Buchbinder, 2016). The BOLD contrast detects these blood flow changes, thereby allowing real-time visualization of brain activity, particularly when performing tasks that require specific cognitive functions (Buchbinder, 2016; Rossi, Nibali, et al., 2019). fMRI is generally used to understand and locate the specific regions of the brain involved in various cognitive processes such as memory, language, and decision-making (Liberta et al., 2020; Nakajima et al., 2018; Prabhakar & Ali, 2019; Sanford & Woodward, 2021). By providing a detailed map of these active areas during cognitive tasks, fMRI aids researchers and clinicians in studying brain function in both healthy and diseased states (Hillis, 2000).

In addition to cognitive mapping, fMRI has significant clinical implications, particularly in neurosurgery (Prabhakar & Ali, 2019). Preoperative fMRI scans allow neurosurgeons to identify brain areas critical cognitive areas, such as those responsible for language and motor functions, and plan surgical approaches that minimize damage to these critical regions (Helmstaedter et al., 2003; Rossi, Sani, et al., 2019). This approach is especially crucial in surgeries involving brain tumors or epileptic foci, where preservation of neurological function is paramount (Helmstaedter et al., 2003; Rossi, Sani, et al., 2019). Furthermore, post-operative fMRI can be used to assess the efficacy of neurorehabilitation interventions by monitoring changes in brain activity patterns over time (Jenkins et al., 2014; Rossi, Nibali, et al., 2019). By quantifying improvements in neural function following rehabilitation, clinicians can tailor treatment strategies to optimize patient outcomes (Jenkins et al., 2014).

fMRI serves as a versatile tool for both research and clinical applications, offering insights into brain function and aiding in the planning and execution of neurosurgical procedures. Its ability to non-invasively map brain activity has revolutionized our understanding of the human brain and has significantly contributed to advancements in neuroimaging and neuroscience (Nakajima et al., 2018; Rossi, Nibali, et al., 2019).

The 11 Cognitive Modes

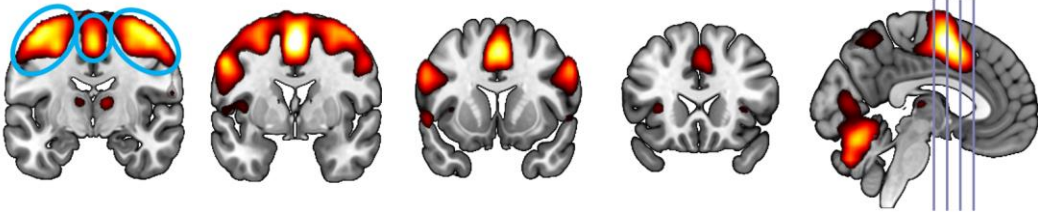
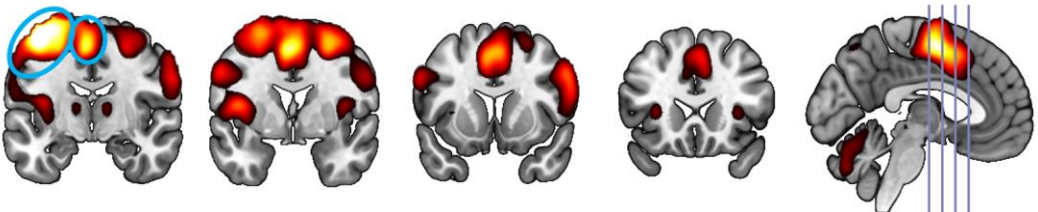

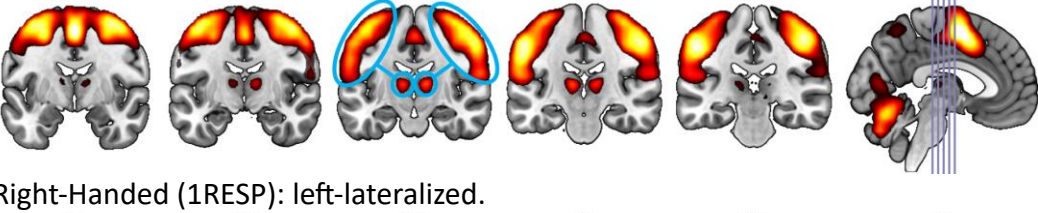


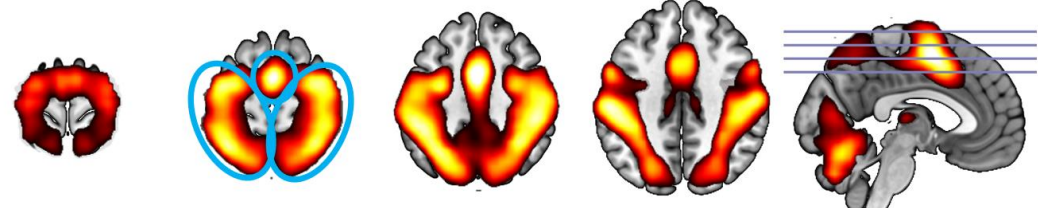

Response (One-Handed 1RESP & Two-Handed 2RESP)

Response (RESP) is a late-peaking mode involved in motor response processes, activating in tasks that require participants to make physical responses (Fouladirad et al., 2022; Sanford et al., 2020; Sanford & Woodward, 2021; Woodward et al., 2013). In terms of timing of task-induced BOLD changes, RESP is observed to be invoked at the onset of the motor response (Fouladirad et al., 2022; Sanford et al., 2020; Sanford & Woodward, 2021; Woodward et al., 2013). It is not load-dependent, such that more difficult task conditions do not generate greater activity (Sanford et al., 2020; Sanford & Woodward, 2021). In tasks where a delay condition exists such that a response is withheld for a brief period, RESP will be suppressed (Passingham & Sakai, 2004; Pasternak & Greenlee, 2005; Sanford et al., 2020; Sanford & Woodward, 2021; Woodward et al., 2013). When a response is not required, RESP is absent (Sanford et al., 2020; Sanford & Woodward, 2021).

Anatomically, RESP involves activity in the medial frontal gyrus, pre-central gyrus, postcentral gyrus, thalamus, superior parietal lobule, cerebellum, and vermis (Percival et al., 2020). These areas of activation form patterns, seen in Table 1, which are: Bat, Thalamus Kite Surfer, Butterfly, and Lobster Claw. For the Bat pattern, we see activation that looks like a bat on coronal slice 10 in the frontal and cingulate; when moving posteriorly through slices 16 to 26, the kite pattern becomes apparent along with the thalamus activity. A butterfly is seen on axial slices 62 and 52 in the postcentral and superior parietal lobule. Continuing inferiorly, on axial slice -24, there is a shape of a lobster with two very large claws on either side in the cerebellum. Two anatomical variations exist based on whether the task design requires a one-handed or two-handed response, and both variations are shown in Table 1. A one-handed response invokes a more prominent activation in the contralateral hemisphere, whereas the two-handed response shows more equal bilateral activation (Percival et al., 2020).

Tasks investigated by our group that activated RESP are working memory (WM) (Sanford, 2019; Sanford et al., 2020; Woodward et al., 2013), visuospatial working memory (Spatial Capacity; SCAP; Sanford, 2019), probabilistic reasoning (Fouladirad et al., 2022), task-switching (Task-Switch Inertia; TSI; Sanford, 2019), and metrical stress (MS) (Besso et al., 2024).

Table 1. Anatomical patterns for the RESP (both two-handed and right-handed).

| | |
|--|---|
| <p>Bat (One Sided if One-Handed Response):</p> <p>Two-Handed (2RESP): bilateral.</p> <p>-10 0 10 20 -3</p>  <p>Right-Handed (1RESP): bat with left wing.</p> <p>-10 0 10 20 -3</p>  |  |
| <p>Thalamus Kite Surfer: on slice 16. Kite becomes more prominent moving from 16 to 26. Kite is more prominent than thalamus activity.</p> <p>Two-Handed (2RESP): bilateral.</p> <p>-6 -11 -16 -21 -26 -3</p>  <p>Right-Handed (1RESP): left-lateralized.</p> <p>-6 -11 -16 -21 -26 -3</p>  |  |
| <p>Butterfly (One Sided if One-Handed Response): mainly on slices 62 and 52.</p> <p>Two-Handed (2RESP): bilateral.</p> <p>72 62 52 42 -3</p>  |  |

Right-Handed (1RESP): left-dominant.

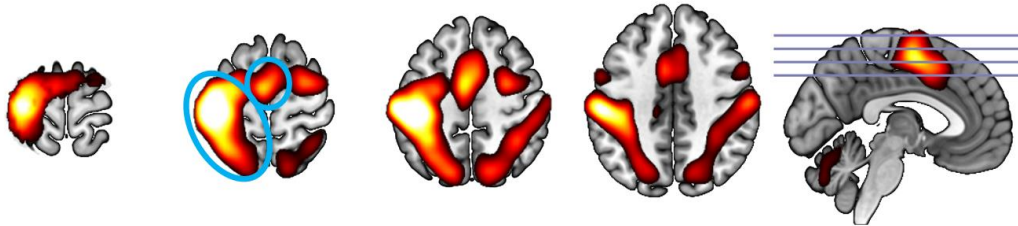
72

62

52

42

-3



Lobster Claw:

Two-Handed (2RESP): bilateral.

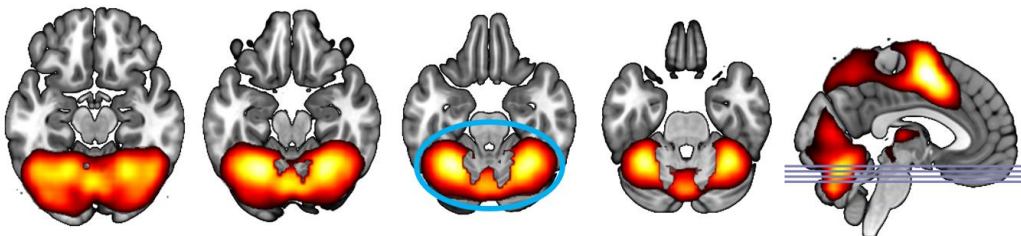
-16

-20

-24

-28

-3



Right-Handed (1RESP): right dominant.

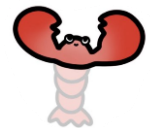
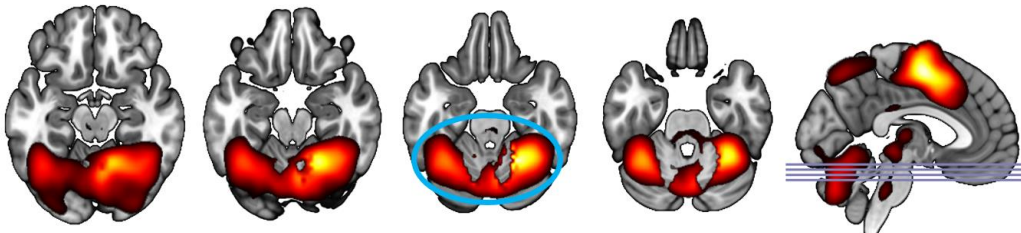
-16

-20

-24

-28

-3






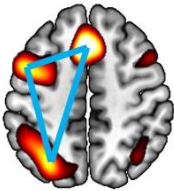
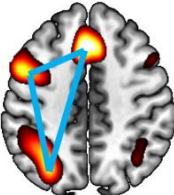
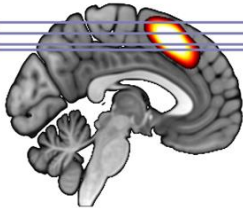



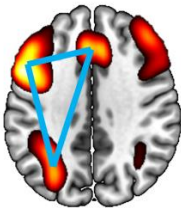
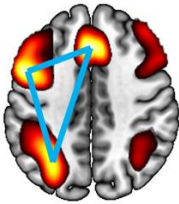
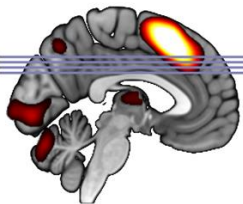



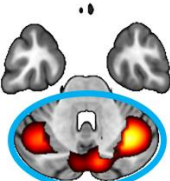

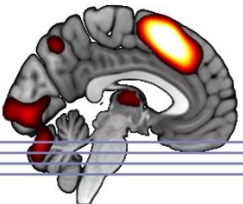


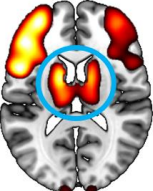
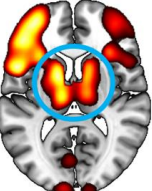
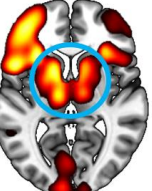
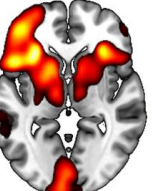
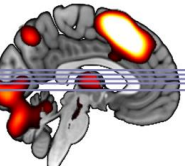
Maintaining Internal Attention (MAIN)

Maintaining Internal Attention (MAIN) is involved in generating or retrieving stored information (Allen et al., 2015; Larivière et al., 2017; Momeni et al., 2024; Sanford et al., 2020; Sanford & Woodward, 2021). It usually peaks mid-trial in tasks where instructions are given to generate or reproduce information (Allen et al., 2015; Larivière et al., 2017; Momeni et al., 2024; Sanford et al., 2020; Sanford & Woodward, 2021). MAIN is highly load-dependent, such that more difficult task conditions will result in greater activation (Allen et al., 2015; Larivière et al., 2017; Momeni et al., 2024; Sanford et al., 2020; Sanford & Woodward, 2021).

Anatomically, the areas of activation include superior frontal gyrus, middle frontal gyrus, medial frontal gyrus, superior parietal lobule, posterior lobule, caudate, lentiform nucleus, sublobar regions, and thalamus (Percival et al., 2020). Using pattern-based classification as pictured in Table 2, MAIN activation patterns include a Left-Lateralized Upper Triangle, Left-Lateralized Lower Triangle, Right-Sided Crab Claw, and Found a Peanut. On axial slices 48, 44, 40, and 36, three prominent regions of activation in the cingulate, frontal, and parietal regions form a triangular shape in the left hemisphere. Moving inferiorly, we see two peanut shapes close to and on either side of the midline posterior to the body of the lateral ventricle, which is slightly left dominant and seen between axial slices 6 to 14. Further inferior to that, there is a right-dominant activity in a crab claw shape apparent in axial slice -32 in the cerebellum.

Tasks published by our group that activated these patterns include the WM task (Sanford, 2019; Sanford et al., 2020), semantic association task (SAT; Eickhoff, 2021; Woodward et al., 2015), autobiographic event simulation (AES) tasks (Momeni et al., 2024), and delusions of reference (DOR) task (Larivière et al., 2017).

Table 2. Anatomical patterns for MAIN.

| | | | | | | |
|---|---|---|---|---|---|---|
| Left-Lateralized Upper Triangle: left-lateralized triangle, see blue lines in slices 44 and 48. | | | | | | |
| 64 | 56 | 48 | 44 | -3 | |  |
|  |  |  |  |  | | |
| Left-Lateralized Lower Triangle: left-lateralized triangle, see blue lines in slices 36 and 40. | | | | | | |
| 28 | 32 | 36 | 40 | -3 | |  |
|  |  |  |  |  | | |
| Right-Sided Crab Claw: right-dominant activity in crab claw formation, most apparent in slice -32. | | | | | | |
| -48 | -40 | -32 | -24 | -3 | |  |
|  |  |  |  |  | | |
| Found a Peanut: two peanuts, slightly left-dominant. | | | | | | |
| 18 | 14 | 10 | 6 | 0 | -3 |  |
|  |  |  |  |  |  | |


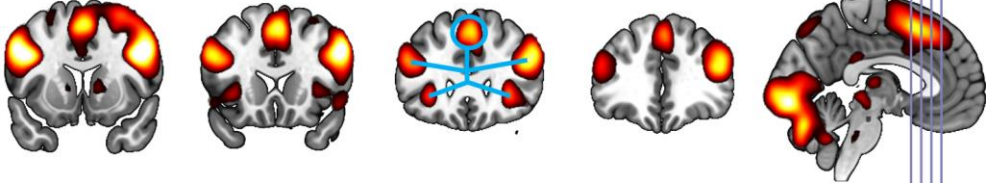

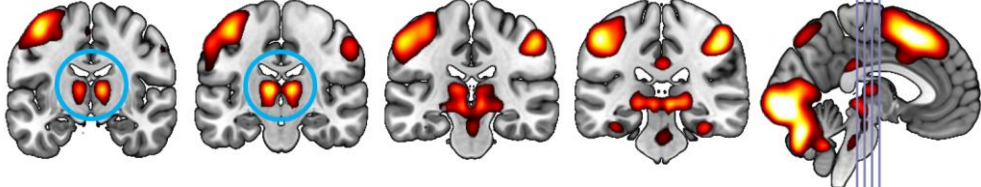

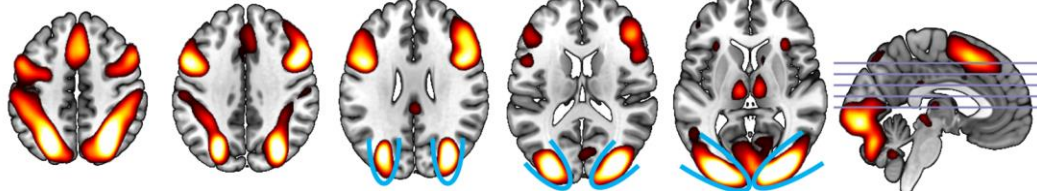

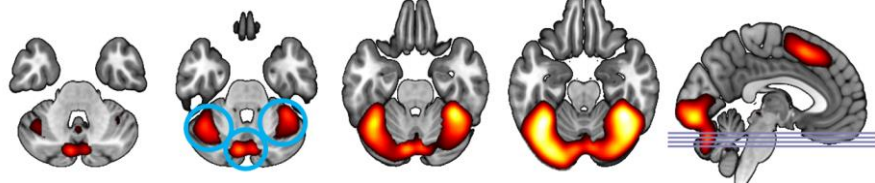
Multiple Demand (MD)

Multiple Demand (MD) is mid-trial peaking hypothesized to be involved in maintaining and directing attention to relevant environmental stimuli, particularly during tasks requiring attention to visual stimuli (Fortenbaugh et al., 2017; Lavigne, Metzak, et al., 2015; Lavigne et al., 2020; Sarter et al., 2001, p. 2020). MD is cognitive load dependent whereby increased levels of cognitive demand or more difficult tasks requiring greater levels of sustained visual attention invoke greater activation (Lavigne et al., 2020).

Anatomically, MD is characterized by activation in the anterior cingulate cortex, bilateral insula, and various sensorimotor regions (Lavigne et al., 2020). Pattern-based classification patterns for MDN are presented in Table 3, and are Jumping Jack Flash, Gorilla Nostrils, Flexing Hands, and Wipe Your Mouth Bear Triple Jam. In Jumping Jack Flash, bilateral activity in the shape of a stick figure involving five prominent regions of activation is seen on coronal slices 18 and/or 26. Moving posteriorly, there is bilateral central activity in the thalamus. Looking at axial slices, we see a Flexing Hands pattern involving bilateral activation in the posterior of the brain, which look like flexing arms on slices 6 to 26. In the cerebellum, there is a pattern resembling jam on the chin and around the side corners of the mouth of a bear, with high jam corners on axial slice -30.

Tasks published by our group that activated MD include MS (Besso et al., 2024), SAT (Eickhoff, 2021; Woodward et al., 2015), probabilistic reasoning (Fouladirad et al., 2022), and behavioral evidence integration (bias against disconfirmatory evidence; BADE; Lavigne et al., 2020).

Table 3. Anatomical patterns for MD.

| | |
|--|---|
| Jumping Jack Flash: bilateral activity in head, hands and feet, prominent on slice 18 and/or 26. |  |
| <p>10 18 26 34 -3</p>  | |
| Gorilla Nostrils: bilateral central activity, prominent on slices -12 or -18. |  |
| <p>-12 -18 -24 -30 -3</p>  | |
| Flexing Hands: bilateral activation on posterior border of slices, hands in slice 26 that begin flexing when moving to slice 6. |  |
| <p>46 36 26 16 6 -3</p>  | |
| Wipe Your Mouth Bear Triple Jam: high jam corners on slice -30. |  |
| <p>-34 -30 -26 -22 -3</p>  | |


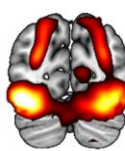
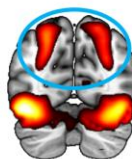
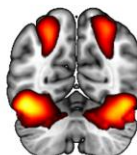
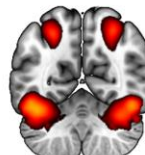
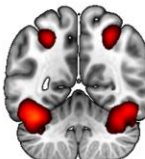
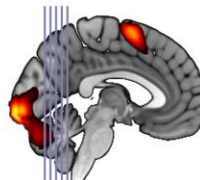
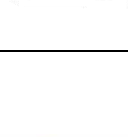

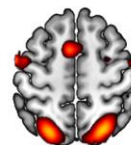
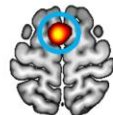

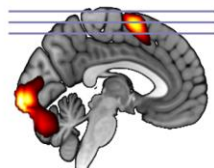

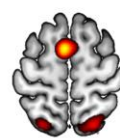




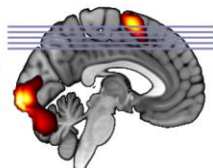
Initiation (INIT)

Initiation (INIT) is an early-peaking mode involved in visual attention that activates during the initiation of trials in tasks involving a non-continuous task procedure with intra-trial pauses (Fouladirad et al., 2022; Sanford et al., 2020; Sanford & Woodward, 2021; Woodward et al., 2013). It is load-dependent whereby more difficult task conditions result in greater activation (Sanford et al., 2020; Sanford & Woodward, 2021; Woodward et al., 2013).

Anatomically, INIT is characterized by activation in the precuneus cortex, superior parietal lobule, supplementary motor area, precentral gyrus, and hippocampus (Percival et al., 2020). Patterns of activation for INIT are Raised Eyebrows, When I'm 64, and De Divina Proportione Front Guy (see Table 4). In Raised Eyebrows, bilateral eyebrow shaped activity is seen on coronal slices -74 and -69 in the precuneus cortex and superior parietal. In When I'm 64, activity peaks on axial slice 64 in the supplementary motor area. In De Devina Proportione Front Guy, five areas of peak activity are seen with left dominance between axial slices 45 through 55.

Tasks published by our group that activated INIT include WM (Sanford, 2019; Sanford et al., 2020; Woodward et al., 2013), TGT (Lavigne, Rapin, et al., 2015, p. 201; Rapin et al., 2012; Sanford, 2019), TSI (Sanford, 2019; Sanford & Woodward, 2021; Woodward et al., 2016), SCAP (Sanford, 2019; Sanford & Woodward, 2021), and probabilistic reasoning (Fouladirad et al., 2022).

Table 4. Anatomical patterns for INIT.

| | | | | | | | |
|---|--|--|--|---|--|---|--|
| Raised Eyebrows: raised bilateral eyebrows in slices -74 and -69. | | | | | | |  |
| -74 | -69 | -64 | -59 | -54 | -3 | | |
|  |  |  |  |  |  |  | |
| When I'm 64: activity peaks on slice 64 not 54. | | | | | | | |
| 54 | 64 | 74 | -3 | | | |  |
|  |  |  |  | | | | |
| De Divina Proportione Front Guy: more prominent on slices 55 and 50. Left hand becomes more prominent in slices 45 through 55. | | | | | | |  |
| 46 | 36 | 26 | 16 | 6 | -3 | | |
|  |  |  |  |  |  | | |




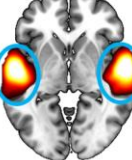
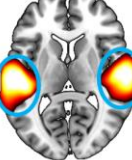


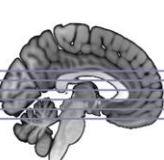


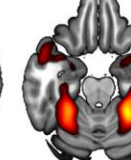
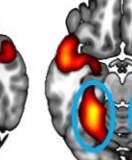
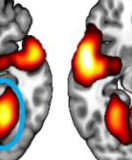
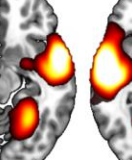
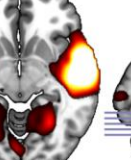
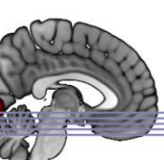
Auditory Perception (AUD)

Auditory Perception (AUD) is mid-trial peaking and involved in auditory processing of complex sounds, such as speech and music (Leaver & Rauschecker, 2010). The activation of AUD sustains until the cessation of the auditory stimulus (Rapin et al., 2012; Sanford et al., 2020; Sanford & Woodward, 2021).

Anatomically, AUD activation is found in the temporal lobe, primary, secondary, and associative visual cortices, hippocampus, and inferior frontal gyrus (Rapin et al., 2012; Sanford et al., 2020; Sanford & Woodward, 2021). Looking at the anatomical patterns in Table 5, Headphones involves prominent bilateral temporal lobe activity in axial slices -2 and 8, and Angry Dragon involves bilateral occipitotemporal area activation in the dragon nose on axial slice -17.

Tasks published by our group that activated AUD were the TGT (Sanford et al., 2020; Sanford & Woodward, 2021) and Radio Speech Task (Gill et al., 2021).

Table 5. Anatomical patterns for AUD.

| | | | | | | | |
|---|---|---|---|---|--|---|---|
| Headphones: prominent bilateral temporal lobe activity in slices -2 and 8. | | | | | | |  |
| -22 | -12 | -2 | 8 | 18 | 28 | -3 | |
|  |  |  |  |  |  |  | |
| Angry Dragon: bilateral occipitotemporal area activation in slice -17. | | | | | | |  |
| -27 | -22 | -17 | -12 | -7 | -3 | | |
|  |  |  |  |  |  |  | |

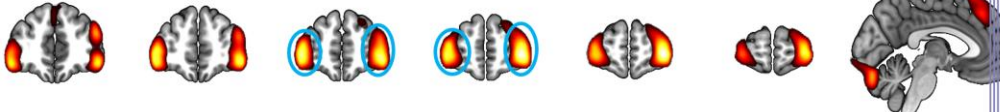
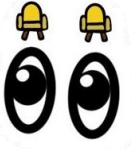
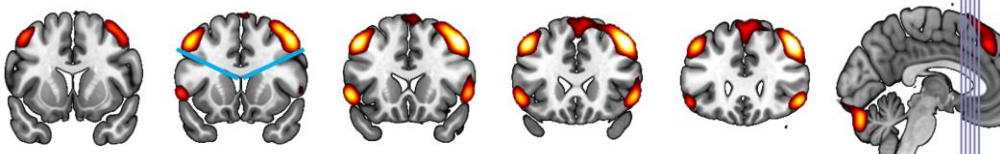
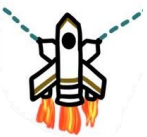
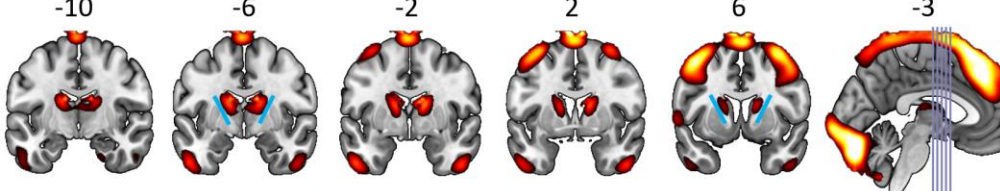

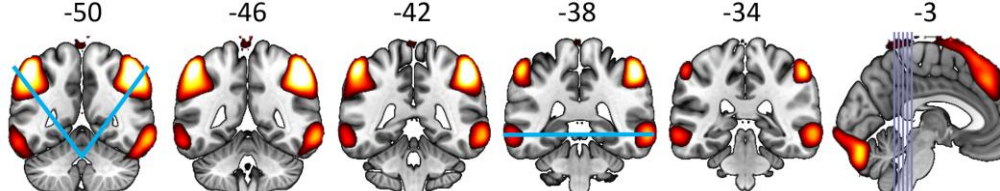

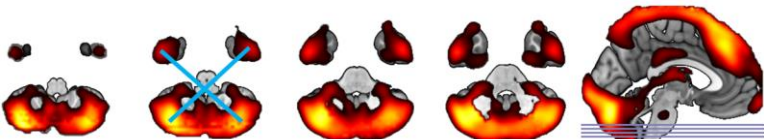

Re-Evaluation (RE-EV)

Re-Evaluation (RE-EV) is late-peaking and is hypothesized to be involved in response evaluation (Lavigne, Metzak, et al., 2015; Lavigne et al., 2020; Sanford, 2019). The peak of activation for RE-EV always occurs after the peak of either RESP in tasks where both RE-EV and RESP are activated, or MDN when RESP is not activated (Lavigne, Metzak, et al., 2015; Lavigne et al., 2020; Sanford, 2019).

Anatomically, RE-EV shows activity in the rostral prefrontal and orbitofrontal cortices, bilateral frontal gyrus, and the superior parietal cortex (Lavigne, Metzak, et al., 2015; Lavigne et al., 2020; Sanford, 2019). In Table 6. using pattern-based classification, bilateral rostral frontal and orbitofrontal activation is seen above the eyeballs in coronal slices 52 and 56. In Bilateral Space Invader Shooters, the activation is seen in the bilateral frontal gyrus at an angle shooting out from the ventricles, prominent in coronal slice 14. In Above the Line (Caudate), there is bilateral activity in the caudate region in coronal slices -6 and 6. For Sad Face Antennae & Flushed Cheeks, there is bilateral activity from the sad mouth (fourth ventricles) that go through eyes (lateral ventricles) and antennae in the parietal cortex on coronal slice -50. The flushed cheeks are in line with the nose (third ventricle) horizontally on coronal slice -38. Lastly, for X Marks the Spot, there is bilateral activation and the X endpoints of axial slices -50 and -46 in the inferior temporal and cerebellum.

Tasks published by our group that activated RE-EV included BADE (Lavigne et al., 2020; Lavigne, Metzak, et al., 2015), TSI (Sanford, 2019), and TGT (Sanford, 2019). The evidence for the proposed cognitive mode for RE-EV involving re-evaluating, re-considering, or regulating mental states is presented in publicly available work (Redway et al., 2024).

Table 6. Anatomical patterns for RE-EV.

| | |
|---|---|
| <p>Bilateral Eyeball Sitters: bilateral activity just above eyeballs.</p> <p>44 48 52 56 60 64 -3</p>  |  |
| <p>Bilateral Space Invader Shooters: the ventricles are shooting bilateral activations, or the activations are just above these projections, see blue lines in slice 14.</p> <p>10 14 18 22 26 -3</p>  |  |
| <p>Above the Line (Caudate): bilateral activity in caudate region, above the blue lines indicated in slice -6 and 6 with blue lines.</p> <p>-10 -6 -2 2 6 -3</p>  |  |
| <p>Sad Face Antennae & Flushed Cheeks: bilateral activity from sad face antennae projections that go from the mouth (fourth ventricle) through the eyes (lateral ventricles), see blue lines in slice -50. Flushed cheeks in line with nose (third ventricle) on slice -38.</p> <p>-50 -46 -42 -38 -34 -3</p>  |  |
| <p>X Marks the Spot: bilateral activation at X endpoints, see blue lines in slices -50 and -46.</p> <p>-50 -46 -42 -38 -3</p>  |  |

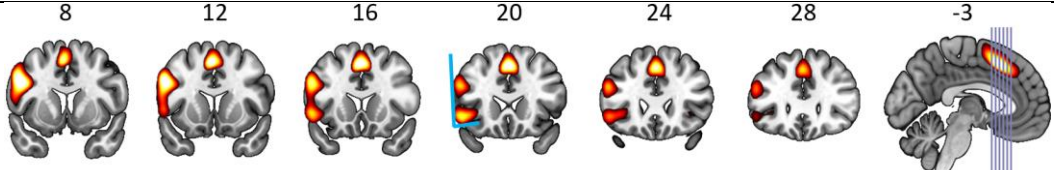

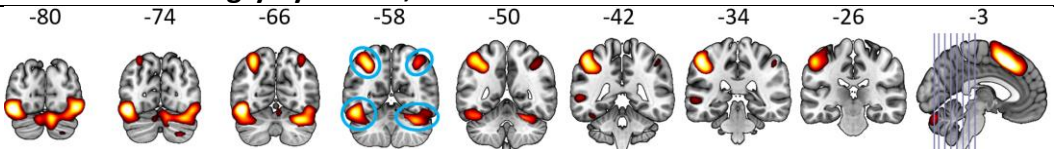

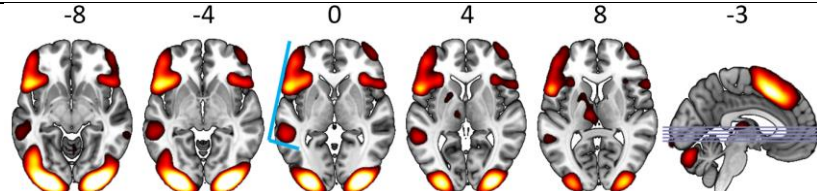

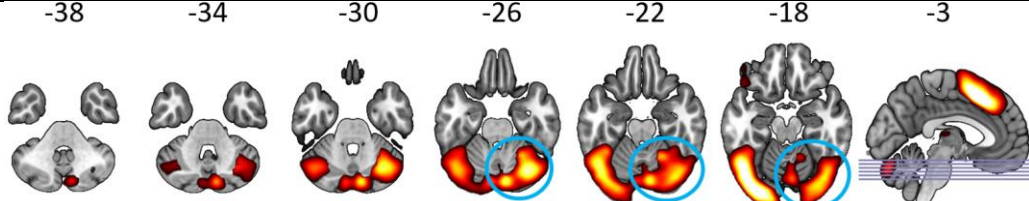

Language (LAN)

Language (LAN) is mid-trial peaking and is involved in linguistic processes such as controlled retrieval/selection of semantic information, and language perception and comprehension. LAN shows load-dependency whereby increased activation occurs with increased linguistic demand, but also shows decreased activation when linguistic information interferes with the task at hand (Goghari et al., 2017a; Kusi et al., 2022; Wong et al., 2020; Woodward et al., 2015).

LAN is characterized by activations in left-dominant regions, including left prefrontal regions (Broca's area), left middle temporal gyrus (BA 22; Wernicke's area), and left angular gyrus (Goghari et al., 2017a; Kusi et al., 2022; Wong et al., 2020; Woodward et al., 2015). The pattern-based activations are shown in Table 7, and are Rail Shot Coronal, Tears Blown Leftwards & Eyebrows, Rail Shot Axial, and Disappearing Face. In Rail Shot Coronal, left lateralized activities with two peaks in the temporal lobe are seen in coronal slice 20. In Tears Blown Leftwards & Eyebrows, teardrops are seen in the fusiform gyrus, as well as eyebrows in the parietal lobe on coronal slices -58 and -50. In Rail Shot Axial, left lateralized activity in the temporal and frontal lobes, including Broca's area. The Disappearing Face shows a diagonal smiley face apparent on the right side on axial slice -18, which becomes left lateralized going down to slice -36 in the cerebellum.

Tasks published by our group that activated LAN included MS (Besso et al., 2024), SAT (Woodward et al., 2015), Lexical Decision Task (LDT; Kusi et al., 2022; Wong et al., 2020), and the Facial Emotion Discrimination (FED) task (Goghari et al., 2017b). The evidence for the proposed cognitive mode for LAN over a wide range of cognitive tasks, which includes both activation and suppression, depending on the linguistic information processing required to achieve the task goals, is presented in publicly available work (Zeng et al., 2024).

Table 7. Anatomical patterns for LAN.

| | |
|---|---|
| <p>Rail Shot Coronal: left lateralized activity, two peaks in line similar to pool rail shot, see blue lines in slice 20.</p>  |  |
| <p>Tears Blown Leftwards & Eyebrows: sad face with teardrop blown leftwards, left-dominant angry eyebrows, see slice -58 and -50.</p>  |  |
| <p>Rail Shot Axial: left lateralized activity, two peaks in line similar to pool rail shot, see blue lines in slice 0.</p>  |  |
| <p>Disappearing Face (Start Right, Disappear Left): diagonal smiley face apparent on right side of slice -18 and disappears by slice -36.</p>  |  |

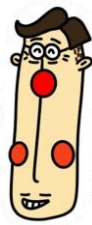
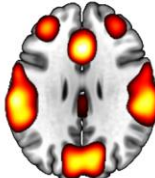


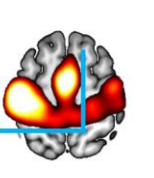
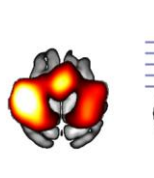
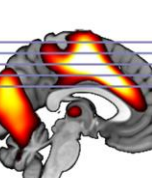

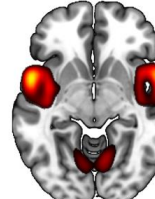
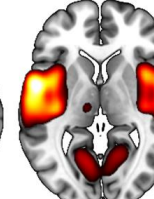
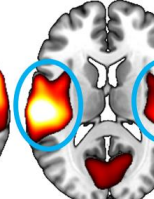
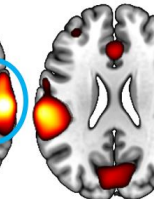
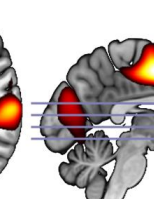

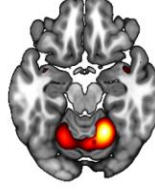
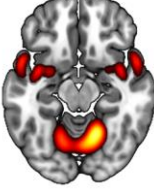

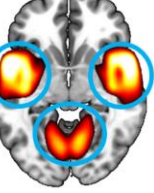
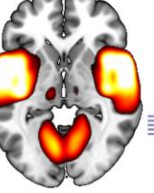
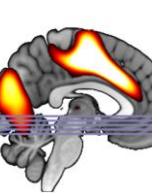
Auditory Attention for Response (AAR)

Auditory Attention for Response (AAR) is mid-trial peaking, and hypothesized to be involved in attention to auditory sounds when a motor response to the auditory stimulus is expected (Lavigne et al., 2016; Lavigne & Woodward, 2018; Sanford & Woodward, 2021). It shows anatomical overlap with AUD (Sanford et al., 2020). AAR appears to show an inverse relationship between auditory and visual stimuli that is cognitive load dependent, whereby tasks requiring greater visual focus results in greater deactivation of AAR (Lavigne et al., 2016; Lavigne & Woodward, 2018; Sanford, 2019).

AAR is characterized by activation in the bilateral superior temporal gyrus, supplementary motor area, left precentral gyrus, bilateral insula and thalamus (Lavigne et al., 2016; Percival et al., 2020). The pattern-based classification patterns are shown in Table 8, and include Happy 28th Birthday Long Face/Right Angle, On Fire, and Small Smile. In Happy 28th Birthday Long Face/Right Angle, a face is seen on axial slice 28 involving activations in the frontal lobe (eyes), cingulate (nose), superior temporal gyrus (cheeks), and calcarine gyrus (mouth). A right angle with left lateralized activity near the central gyrus and cingulate is seen on axial slice 58. In On Fire, flame shapes on axial slice 13 is seen bilaterally in the temporal lobes. In Small Smile, small eyes (insula) and smile (lingual gyrus) dominate on axial slices -10 and -6.

Tasks published by our group that activated AAR included the TGT (Lavigne & Woodward, 2018), auditory oddball (Kim et al., 2009; Lavigne et al., 2016), SM (Eickhoff, 2021), and SAT (Eickhoff, 2021).

Table 8. Anatomical patterns for AAR.

| | | | | | | |
|---|--|--|--|---|--|--|
| Happy 28th Birthday Long Face/Right Angle: slice 28 has long face with cheeks. Right angle on slice 58. | | | | | |  |
| 28 | 38 | 48 | 58 | 68 | -3 | |
|  |  |  |  |  |  | |
| On Fire: flame shapes on slice 13 bilaterally in the temporal lobes. | | | | | |  |
| -7 | 3 | 13 | 23 | -3 | | |
|  |  |  |  |  | | |
| Small Smile: small eyes and smile dominant on slices -10 and -6. | | | | | |  |
| -18 | -14 | -10 | -6 | -2 | -3 | |
|  |  |  |  |  |  | |

Focus on Visual Features (FoVF)

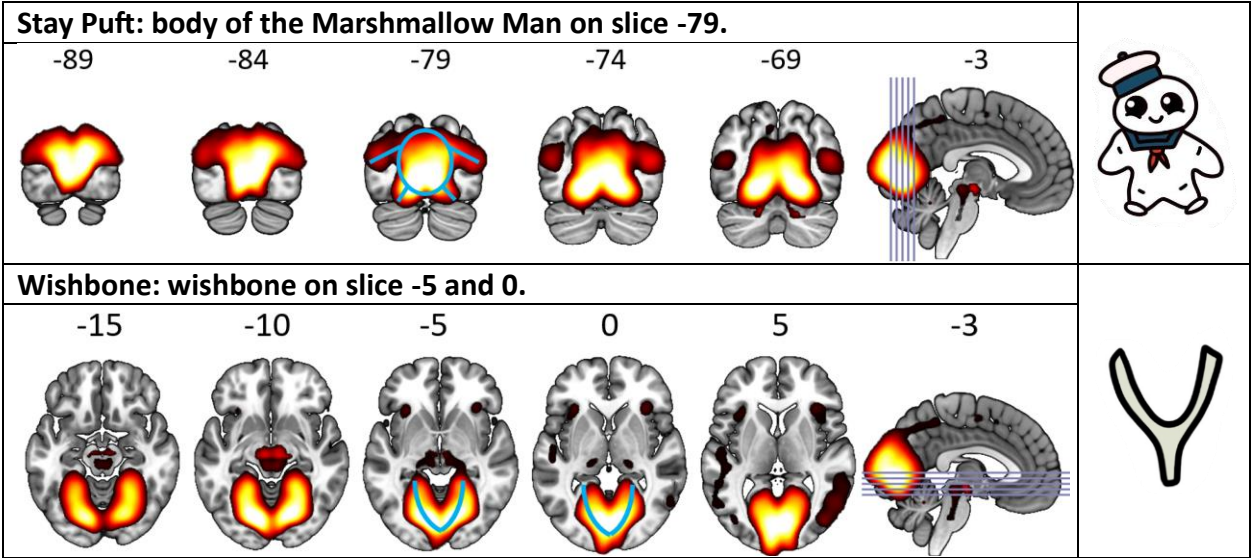
Focus on Visual Features (FoVF) is involved in attention to the visual features of complex visual stimuli, and timing of activation corresponds to visual stimuli presentation during the trial (Gill et al., 2021, p. 2; Lavigne, Metzack, et al., 2015; Sanford et al., 2020; Woodward et al., 2013).

FoVF may be deactivated in tasks with visual stimuli where the features of the image (for example, type font or word size) are not the focus, possibly to redirect attention to what the image is representing (for example, what the word or letters symbolize) (Sanford et al., 2020; Sanford & Woodward, 2021; Woodward et al., 2013)

AAR is characterized by a reciprocal relationship between activity in the lateral occipital cortex and the medial occipital and parietal cortex, possibly tracing the BOLD fluctuations between the primary and secondary visual cortices (Sanford et al., 2020). The patterns of activation are seen in Table 9, and are Stay Puft and Wishbone. In Stay Puft, occipital cortex activation is seen in the shape of a body of the Marshmallow Man on coronal slice -79. In Wishbone, activations in the fusiform and lingual gyri form a wishbone shape.

Tasks published by our group that activated FoVF included during visual stimuli presentation in TGT (Sanford et al., 2020) and BADE (Lavigne, Metzack, et al., 2015) and deactivated in WM (Sanford et al., 2020; Woodward et al., 2013) and TSI (Sanford, 2019) during presentation of letters/words.

Table 9. Anatomical patterns for FoVF.



Default Mode A (DMA)


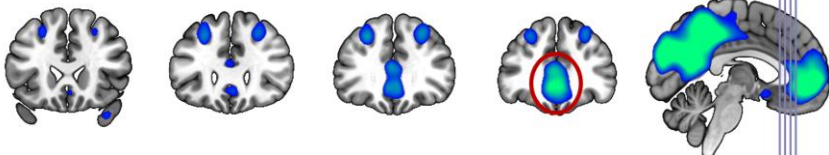

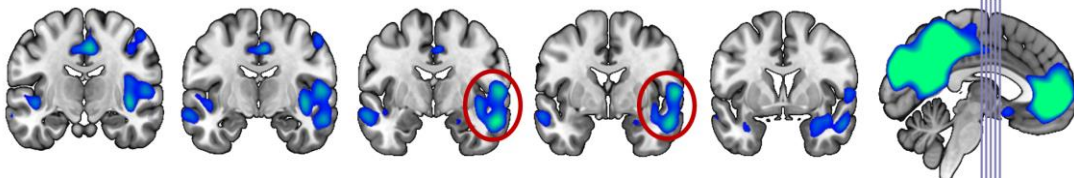

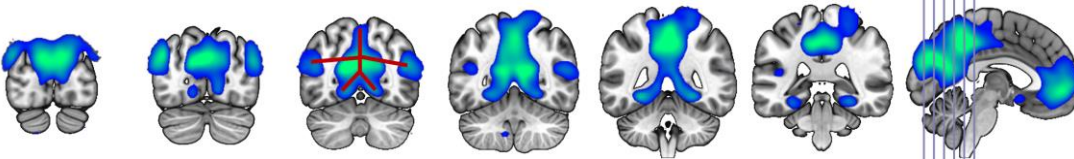

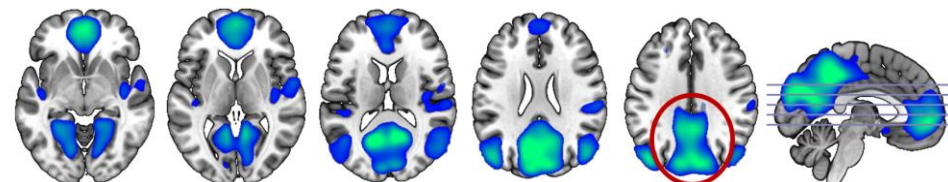

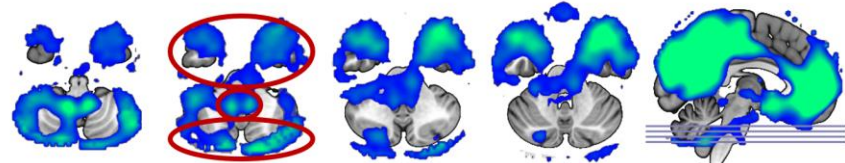

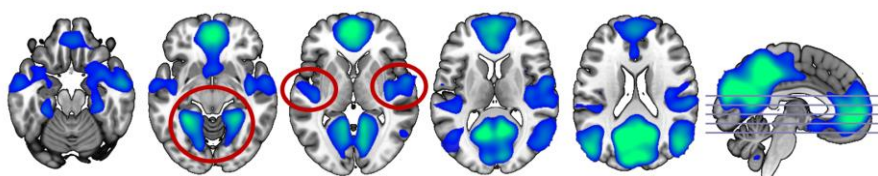
The two default modes anatomically involve discrete cortical areas such as the ventral medial prefrontal cortex, precuneus cortex, angular gyrus, and the superior frontal gyrus (Buckner et al., 2008; Harrison et al., 2008). DM uses increased metabolic activity at rest and decreased activity during goal-oriented tasks, contrasting the other frontal and parietal cortical regions (Fox et al., 2005; Raichle et al., 2001).

The DMA appears to be mid-to-late trial peaking and is cognitive load-dependent, showing more pronounced activation (or more brain deactivation) during more demanding tasks (Enz, 2019). DMA is negatively related to language processing, (LAN) internal attention (MAIN), and re-evaluation (RE-EV), showing decreased activation when these cognitive demands interfere with the task at hand (Du et al., 2023; Enz, 2019).

The DMA is characterized by deactivation in regions such as the posterior parahippocampal cortex (PHC), retrosplenial cortex (RSC), ventral posterior cingulate cortex (PCC), precuneus, cuneal cortex, and lingual gyrus (Du et al., 2023; Percival et al., 2020). Looking at the pattern-based classification patterns in Table 10, DMA shows a Snowman Mouth on coronal slice 37 with lower deactivation compared to DMB (see Table 11 for DMB patterns). In Muted Medial Temporal Dots, the DMA shows muted right-dominant dots of deactivation in the medial temporal lobe on coronal slices -2 and -6, compared to more prominent and bilateral temporal dots in DMB. On coronal slice -66, a penguin figure is seen with low shoulders and chest in the parieto-occipital and temporal lobes and lingual gyrus. On axial slice 34, the Kitten pattern is seen in the parietooccipital lobe deactivation. Inferiorly, on axial slice -42, a Laughing Clown pattern of deactivation is seen in the temporal lobe and cerebellum. Lastly, in You're In Trouble, an unpleased human is seen with fists on their hips with prominent feet in axial slices -10 and 0 from deactivations in the parietooccipital and lingual gyrus, and forearms at the angular gyrus.

Tasks published by our group that activated the DMA include MS and SAT (Enz, 2019).

Table 10. Anatomical patterns for DMA.

| | |
|--|---|
| Snowman Mouth: slice 37 with lower deactivation “mouth” compared to “nose” in DMB. |  |
| <p>22 27 32 37 -3</p>  | |
| Muted Medial Temporal Dots: muted right-dominant medial temporal dots. |  |
| <p>-14 -10 -6 -2 2 -3</p>  | |
| Penguin: low shoulders and chest on slice -66. More prominent chest than arms. |  |
| <p>-86 -76 -66 -56 -46 -36 -3</p>  | |
| Kitten: the kitten is sitting facing into the screen. |  |
| <p>-6 4 14 24 34 -3</p>  | |
| Laughing Clown: |  |
| <p>-47 -42 -37 -32 -3</p>  | |
| You're In Trouble: prominent feet in slices -10 and 0. Basal ganglia arms. Forearms and elbows more anterior and medial, particularly in slice 0. |  |
| <p>-20 -10 0 10 20 -3</p>  | |

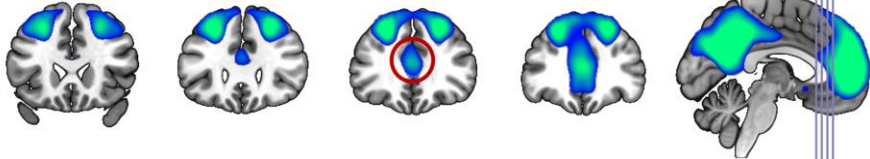

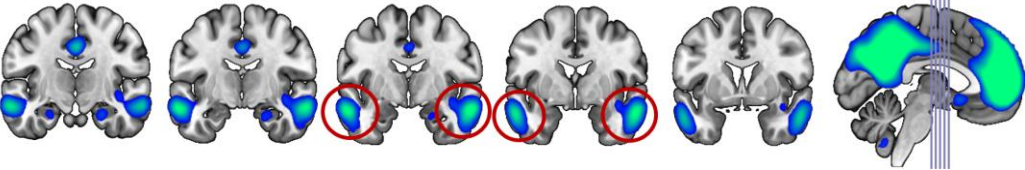

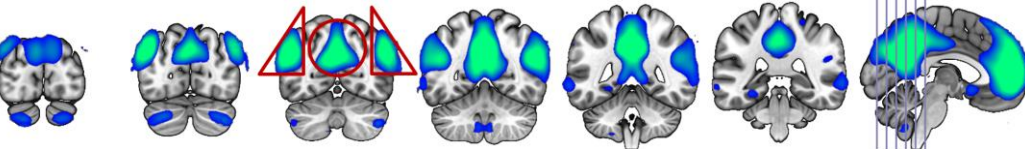

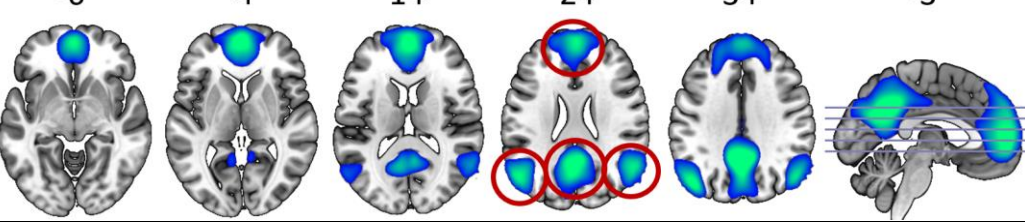

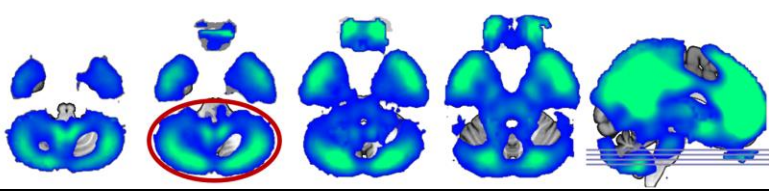

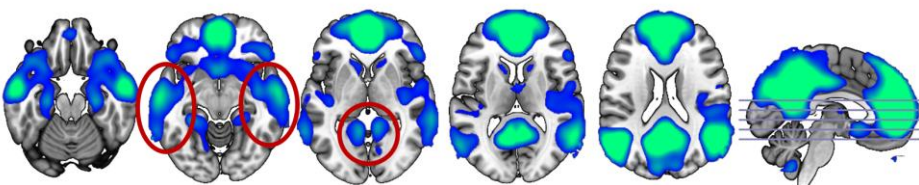

Default Mode B (DMB)

The Default Mode B (DMB) is typically deactivated during tasks that necessitate external attention and cognitive engagement, illustrating its negative relationship with task-positive modes such as the external attention (EXT) and response (RESP) (Lavigne, Metzak, et al., 2015; Metzak et al., 2011; Sanford, 2019; Sanford et al., 2020; Woodward et al., 2016). Generally, DMB deactivates in response to task engagement and shows significant activity during early-to-mid parts of the trial that is cognitive-load dependent, such that more difficult task conditions elicit greater activation (Lavigne, Metzak, et al., 2015; Metzak et al., 2011; Sanford, 2019; Sanford et al., 2020; Woodward et al., 2016).

Core areas of DMB activity include the superior frontal gyrus and lateral occipital cortex (Du et al., 2023; Percival et al., 2020). Pattern-based classification patterns are depicted in Table 11. In coronal slice 32, deactivation is seen more superiorly in the brain forming a nose shape, compared to a more inferior activation seen in DMA (shown in Table 10). Prominent bilateral medial temporal deactivations are seen in coronal slices -2 and -6. Moving posteriorly, an In Flight bird pattern is seen with prominent wing shaped activity on coronal slice -66 in the temporal lobe; the bird wings are high and in line with the head, which differs from the Penguin pattern in DMA. In the Tripod pattern, deactivations are seen mostly on axial slices 24 and 34 in the frontal, temporal, and precuneus areas. Moving inferiorly, Mandibles are seen in the cerebellum on axial slice -42. Lastly, on axial slices -10 and 0, less prominent feet are seen in the Angel Wings pattern compared to You're In Trouble in DMA. Additionally, the wingtips are more posterior and lateral in the temporal lobes compared to the forearms in You're In Trouble, particularly on axial slice 0.

Tasks published by our group that activated/deactivated the DMB include the BADE (Lavigne & Woodward, 2018), WM (Sanford, 2019; Sanford et al., 2020), SCAP (Sanford, 2019), TSI (Sanford, 2019; Woodward et al., 2016), TGT (Sanford, 2019; Sanford & Woodward, 2021), LDT (Wong et al., 2020), MS (Besso et al., 2024), SAT (Eickhoff, 2021), AES (Momeni et al., 2024), and probabilistic reasoning tasks (Fouladirad et al., 2022).

Table 11. Anatomical patterns for the DMB.

| | |
|--|---|
| <p>Snowman Nose: slice 32 with middle deactivation “nose” compared to “mouth” in DMA.</p> <p>22 27 32 37 -3</p>  |  |
| <p>Prominent bilateral medial temporal dots.</p> <p>-14 -10 -6 -2 2 -3</p>  |  |
| <p>In Flight: prominent bilateral wing shaped activity.</p> <p>-86 -76 -66 -56 -46 -36 -3</p>  |  |
| <p>Tripod: mostly on slices 24 and 34.</p> <p>-6 4 14 24 34 -3</p>  |  |
| <p>Mandibles: take threshold right down to -.1 and -.01.</p> <p>-47 -42 -37 -32 -3</p>  |  |
| <p>Angel Wings: feet less prominent in slices -10 and 0. Basal ganglia wings. Wingtips more posterior and lateral, particular in slice 0.</p> <p>-20 -10 0 10 20 -3</p>  |  |

References

- Allen, P., Chaddock, C. A., Egerton, A., Howes, O. D., Barker, G., Bonoldi, I., Fusar-Poli, P., Murray, R., & McGuire, P. (2015). Functional Outcome in People at High Risk for Psychosis Predicted by Thalamic Glutamate Levels and Prefronto-Striatal Activation. *Schizophrenia Bulletin*, 41(2), 429–439. <https://doi.org/10.1093/schbul/sbu115>
- Besso, L., Larivière, S., Roes, M., Sanford, N., Percival, C., Damascelli, M., Momeni, A., Lavigne, K., Menon, M., Aleman, A., Ćurčić-Blake, B., & Woodward, T. S. (2024). Hypoactivation of the language network during auditory imagery contributes to hallucinations in Schizophrenia. *Psychiatry Research: Neuroimaging*, 341, 111824. <https://doi.org/10.1016/j.psychresns.2024.111824>
- Buchbinder, B. R. (2016). Functional magnetic resonance imaging. In *Handbook of Clinical Neurology* (Vol. 135, pp. 61–92). Elsevier. <https://doi.org/10.1016/B978-0-444-53485-9.00004-0>
- Buckner, R. L., Andrews-Hanna, J. R., & Schacter, D. L. (2008). The Brain's Default Network. *Annals of the New York Academy of Sciences*, 1124(1), 1–38. <https://doi.org/10.1196/annals.1440.011>
- Cattell, R. B. (1966). The Scree Test For The Number Of Factors. *Multivariate Behavioral Research*, 1(2), 245–276. https://doi.org/10.1207/s15327906mbr0102_10
- Cattell, R. B., & Vogelman, S. (1977). A Comprehensive Trial Of The Scree And Kg Criteria For Determining The Number Of Factors. *Multivariate Behavioral Research*, 12(3), 289–325. https://doi.org/10.1207/s15327906mbr1203_2
- Ćurčić-Blake, B., Liemburg, E., Vercammen, A., Swart, M., Knegtering, H., Bruggeman, R., & Aleman, A. (2013). When Broca Goes Uninformed: Reduced Information Flow to Broca's Area in Schizophrenia Patients With Auditory Hallucinations. *Schizophrenia Bulletin*, 39(5), 1087–1095. <https://doi.org/10.1093/schbul/sbs107>
- Du, J., DiNicola, L. M., Angeli, P. A., Saadon-Grosman, N., Sun, W., Kaiser, S., Ladopoulou, J., Xue, A., Yeo, B. T. T., Eldaief, M. C., & Buckner, R. L. (2023). *Within-Individual Organization of the Human Cerebral Cortex: Networks, Global Topography, and Function*. <https://doi.org/10.1101/2023.08.08.552437>
- Durda, K., Buchanan, L. (2006). *WordMine2* [Online] Available: <http://web2.uwindsor.ca/wordmine>
- Eickhoff, S. (2021). *The Association of Brain Networks common to Source monitoring and Semantic Integration with the Symptoms of Schizophrenia*. Universität zu Lübeck.
- Enz, R. (2019). *Identifying Impairment in Task-Related Functional Brain Networks in Schizophrenia*.
- Fortenbaugh, F. C., DeGutis, J., & Esterman, M. (2017). Recent theoretical, neural, and clinical advances in sustained attention research. *Annals of the New York Academy of Sciences*, 1396(1), 70–91. <https://doi.org/10.1111/nyas.13318>
- Fouladirad, S., Chen, L. V., Roes, M., Chinchani, A., Percival, C., Khangura, J., Zahid, H., Moscovitz, A., Arreaza, L., Wun, C., Sanford, N., Balzan, R., Moritz, S., Menon, M., & Woodward, T. S. (2022). Functional brain networks underlying probabilistic reasoning and delusions in schizophrenia. *Psychiatry Research: Neuroimaging*, 323, 111472. <https://doi.org/10.1016/j.psychresns.2022.111472>

- Fox, M. D., Snyder, A. Z., Vincent, J. L., Corbetta, M., Van Essen, D. C., & Raichle, M. E. (2005). The human brain is intrinsically organized into dynamic, anticorrelated functional networks. *Proceedings of the National Academy of Sciences*, 102(27), 9673–9678. <https://doi.org/10.1073/pnas.0504136102>
- Gill, K., Percival, C., Roes, M., Arreaza, L., Chinchani, A., Sanford, N., Sena, W., Mohammadsadeghi, H., Menon, M., Hughes, M., Carruthers, S., Sumner, P., Woods, W., Jardri, R., Sommer, I. E., Rossell, S. L., & Woodward, T. S. (2021). *Brain Networks Detectable by fMRI during On-Line Self Report of Hallucinations in Schizophrenia* (p. 2021.11.06.467564). bioRxiv. <https://doi.org/10.1101/2021.11.06.467564>
- Goghari, V. M., Sanford, N., Spilka, M. J., & Woodward, T. S. (2017a). Task-Related Functional Connectivity Analysis of Emotion Discrimination in a Family Study of Schizophrenia. *Schizophrenia Bulletin*, 43(6), 1348–1362. <https://doi.org/10.1093/schbul/sbx004>
- Goghari, V. M., Sanford, N., Spilka, M. J., & Woodward, T. S. (2017b). Task-Related Functional Connectivity Analysis of Emotion Discrimination in a Family Study of Schizophrenia. *Schizophrenia Bulletin*, 43(6), 1348–1362. <https://doi.org/10.1093/schbul/sbx004>
- Gordon, E. M., Laumann, T. O., Gilmore, A. W., Newbold, D. J., Greene, D. J., Berg, J. J., Ortega, M., Hoyt-Drazen, C., Gratton, C., Sun, H., Hampton, J. M., Coalson, R. S., Nguyen, A. L., McDermott, K. B., Shimony, J. S., Snyder, A. Z., Schlaggar, B. L., Petersen, S. E., Nelson, S. M., & Dosenbach, N. U. F. (2017). Precision Functional Mapping of Individual Human Brains. *Neuron*, 95(4), 791–807.e7. <https://doi.org/10.1016/j.neuron.2017.07.011>
- Harrison, B. J., Pujol, J., López-Solà, M., Hernández-Ribas, R., Deus, J., Ortiz, H., Soriano-Mas, C., Yücel, M., Pantelis, C., & Cardoner, N. (2008). Consistency and functional specialization in the default mode brain network. *Proceedings of the National Academy of Sciences*, 105(28), 9781–9786. <https://doi.org/10.1073/pnas.0711791105>
- Helmstaedter, C., Kurthen, M., Lux, S., Reuber, M., & Elger, C. E. (2003). Chronic epilepsy and cognition: A longitudinal study in temporal lobe epilepsy. *Annals of Neurology*, 54(4), 425–432. <https://doi.org/10.1002/ana.10692>
- Hillis, A. E. (2000). Cognitive impairments after surgical repair of ruptured and unruptured aneurysms. *Journal of Neurology, Neurosurgery & Psychiatry*, 69(5), 608–615. <https://doi.org/10.1136/jnnp.69.5.608>
- Hunter, M. A., & Takane, Y. (2002). Constrained Principal Component Analysis: Various Applications. *Journal of Educational and Behavioral Statistics*, 27(2), 105–145. <https://doi.org/10.3102/10769986027002105>
- Jenkins, L. M., Andrewes, D. G., Nicholas, C. L., Drummond, K. J., Moffat, B. A., Phal, P., Desmond, P., & Kessels, R. P. C. (2014). Social cognition in patients following surgery to the prefrontal cortex. *Psychiatry Research: Neuroimaging*, 224(3), 192–203. <https://doi.org/10.1016/j.psychresns.2014.08.007>
- Kim, D. I., Mathalon, D. H., Ford, J. M., Mannell, M., Turner, J. A., Brown, G. G., Belger, A., Gollub, R., Lauriello, J., Wible, C., O’Leary, D., Lim, K., Toga, A., Potkin, S. G., Birn, F., & Calhoun, V. D. (2009). Auditory Oddball Deficits in Schizophrenia: An Independent Component Analysis of the fMRI Multisite Function BIRN Study. *Schizophrenia Bulletin*, 35(1), 67–81. <https://doi.org/10.1093/schbul/sbn133>
- Kiss, G. (1973). In *An associative thesaurus of English and its computer analysis* (p. 165). University Press.

- Knecht, S., Dräger, B., Deppe, M., Bobe, L., Lohmann, H., Flöel, A., Ringelstein, E.-B., & Henningsen, H. (2000). Handedness and hemispheric language dominance in healthy humans. *Brain*, 123(12), 2512–2518. <https://doi.org/10.1093/brain/123.12.2512>
- Kusi, M., Wong, S. T. S., Percival, C. M., Zurrin, R., Roes, M. M., Woodward, T. S., & Goghari, V. M. (2022). Altered activity in functional brain networks involved in lexical decision making in bipolar disorder: An fMRI case-control study. *Journal of Affective Disorders*, 317, 59–71. <https://doi.org/10.1016/j.jad.2022.08.040>
- Larivière, S., Lavigne, K. M., Woodward, T. S., Gerretsen, P., Graff-Guerrero, A., & Menon, M. (2017). Altered functional connectivity in brain networks underlying self-referential processing in delusions of reference in schizophrenia. *Psychiatry Research: Neuroimaging*, 263, 32–43. <https://doi.org/10.1016/j.psychres.2017.03.005>
- Lavigne, K. M., Menon, M., & Woodward, T. S. (2016). Impairment in subcortical suppression in schizophrenia: Evidence from the fBIRN Oddball Task. *Human Brain Mapping*, 37(12), 4640–4653. <https://doi.org/10.1002/hbm.23334>
- Lavigne, K. M., Menon, M., & Woodward, T. S. (2020). Functional Brain Networks Underlying Evidence Integration and Delusions in Schizophrenia. *Schizophrenia Bulletin*, 46(1), 175–183. <https://doi.org/10.1093/schbul/sbz032>
- Lavigne, K. M., Metzak, P. D., & Woodward, T. S. (2015). Functional brain networks underlying detection and integration of disconfirmatory evidence. *NeuroImage*, 112, 138–151. <https://doi.org/10.1016/j.neuroimage.2015.02.043>
- Lavigne, K. M., Rapin, L. A., Metzak, P. D., Whitman, J. C., Jung, K., Dohen, M., Løevenbruck, H., & Woodward, T. S. (2015). Left-Dominant Temporal-Frontal Hypercoupling in Schizophrenia Patients With Hallucinations During Speech Perception. *Schizophrenia Bulletin*, 41(1), 259–267. <https://doi.org/10.1093/schbul/sbu004>
- Lavigne, K. M., & Woodward, T. S. (2018). Hallucination- and speech-specific hypercoupling in frontotemporal auditory and language networks in schizophrenia using combined task-based fMRI data: An fBIRN study. *Human Brain Mapping*, 39(4), 1582–1595. <https://doi.org/10.1002/hbm.23934>
- Leaver, A. M., & Rauschecker, J. P. (2010). Cortical Representation of Natural Complex Sounds: Effects of Acoustic Features and Auditory Object Category. *The Journal of Neuroscience*, 30(22), 7604–7612. <https://doi.org/10.1523/JNEUROSCI.0296-10.2010>
- Liberta, T. A., Kagiwada, M., Ho, K., Spat-Lemus, J., Voelbel, G., Kohn, A., Perrine, K., Josephs, L., McLean, E. A., & Sacks-Zimmerman, A. (2020). An investigation of Cogmed working memory training for neurological surgery patients. *Interdisciplinary Neurosurgery*, 21, 100786. <https://doi.org/10.1016/j.inat.2020.100786>
- Metzak, P. D., Feredoes, E., Takane, Y., Wang, L., Weinstein, S., Cairo, T., Ngan, E. T. C., & Woodward, T. S. (2011). Constrained principal component analysis reveals functionally connected load-dependent networks involved in multiple stages of working memory. *Human Brain Mapping*, 32(6), 856–871. <https://doi.org/10.1002/hbm.21072>
- Metzak, P. D., Riley, J. D., Wang, L., Whitman, J. C., Ngan, E. T. C., & Woodward, T. S. (2012). Decreased Efficiency of Task-Positive and Task-Negative Networks During Working Memory in Schizophrenia. *Schizophrenia Bulletin*, 38(4), 803–813. <https://doi.org/10.1093/schbul/sbq154>

- Momeni, A., Addis, D. R., Feredoes, E., Klepel, F., Rasheed, M., Chinchani, A., & Woodward, T. (2024). *Functional Brain Networks Underlying Autobiographical Event Simulation: An Update*. PsyArXiv, June 3, <https://doi.org/10.31219/osf.io/3s69b>
- Nakajima, R., Yordanova, Y. N., Duffau, H., & Herbet, G. (2018). Neuropsychological evidence for the crucial role of the right arcuate fasciculus in the face-based mentalizing network: A disconnection analysis. *Neuropsychologia*, 115, 179–187. <https://doi.org/10.1016/j.neuropsychologia.2018.01.024>
- Passingham, D., & Sakai, K. (2004). The prefrontal cortex and working memory: Physiology and brain imaging. *Current Opinion in Neurobiology*, 14(2), 163–168. <https://doi.org/10.1016/j.conb.2004.03.003>
- Pasternak, T., & Greenlee, M. W. (2005). Working memory in primate sensory systems. *Nature Reviews Neuroscience*, 6(2), 97–108. <https://doi.org/10.1038/nrn1603>
- Percival, C. M., Zahid, H. B., & Woodward, T. S. (2020). *CNoS-Lab/Woodward_Atlas* [Computer software]. Zenodo. <https://doi.org/10.5281/zenodo.4281551>
- Prabhakar, H., & Ali, Z. (Eds.). (2019). *Textbook of Neuroanesthesia and Neurocritical Care: Volume I - Neuroanesthesia*. Springer Singapore. <https://doi.org/10.1007/978-981-13-3387-3>
- Raichle, M. E., MacLeod, A. M., Snyder, A. Z., Powers, W. J., Gusnard, D. A., & Shulman, G. L. (2001). A default mode of brain function. *Proceedings of the National Academy of Sciences*, 98(2), 676–682. <https://doi.org/10.1073/pnas.98.2.676>
- Rapin, L. A., Dohen, M., Løevenbruck, H., Whitman, J. C., Metzack, P. D., & Woodward, T. S. (2012). Hyperintensity of functional networks involving voice-selective cortical regions during silent thought in schizophrenia. *Psychiatry Research: Neuroimaging*, 202(2), 110–117. <https://doi.org/10.1016/j.psychres.2011.12.014>
- Redway, S., Arreaza, L., Shahki, J., Zeng, E., & Woodward, T. (2024). The Pattern-Based Anatomy and Cognitive Mode associated with the Re-Evaluation (RE-EV) Network in fMRI. PsyArXiv. June 27. <https://doi.org/10.31234/osf.io/y7pv2>
- Rossi, M., Nibali, M. C., Torregrossa, F., Bello, L., & Grasso, G. (2019). Innovation in Neurosurgery: The Concept of Cognitive Mapping. *World Neurosurgery*, 131, 364–370. <https://doi.org/10.1016/j.wneu.2019.06.177>
- Rossi, M., Sani, S., Nibali, M. C., Forna, L., Bello, L., & Byrne, R. W. (2019). Mapping in Low-Grade Glioma Surgery. *Neurosurgery Clinics of North America*, 30(1), 55–63. <https://doi.org/10.1016/j.nec.2018.08.003>
- Sanford, N. (2019). *Functional brain networks underlying working memory performance in schizophrenia: A multi-experiment approach*.
- Sanford, N., Whitman, J. C., & Woodward, T. S. (2020). Task-merging for finer separation of functional brain networks in working memory. *Cortex*, 125, 246–271. <https://doi.org/10.1016/j.cortex.2019.12.014>
- Sanford, N., & Woodward, T. S. (2021). Functional Delineation of Prefrontal Networks Underlying Working Memory in Schizophrenia: A Cross-data-set Examination. *Journal of Cognitive Neuroscience*, 33(9), 1880–1908. https://doi.org/10.1162/jocn_a_01726
- Sarter, M., Givens, B., & Bruno, J. P. (2001). The cognitive neuroscience of sustained attention: Where top-down meets bottom-up. *Brain Research Reviews*, 35(2), 146–160. [https://doi.org/10.1016/S0165-0173\(01\)00044-3](https://doi.org/10.1016/S0165-0173(01)00044-3)

- Takane, Y., & Hunter, M. A. (2001). Constrained Principal Component Analysis: A Comprehensive Theory. *Applicable Algebra in Engineering, Communication and Computing*, 12(5), 391–419. <https://doi.org/10.1007/s002000100081>
- Whitman, J. C., Metzak, P. D., Lavigne, K. M., & Woodward, T. S. (2013). Functional connectivity in a frontoparietal network involving the dorsal anterior cingulate cortex underlies decisions to accept a hypothesis. *Neuropsychologia*, 51(6), 1132–1141. <https://doi.org/10.1016/j.neuropsychologia.2013.02.016>
- Wong, S. T. S., Goghari, V. M., Sanford, N., Lim, R., Clark, C., Metzak, P. D., Rossell, S. L., Menon, M., & Woodward, T. S. (2020). Functional brain networks involved in lexical decision. *Brain and Cognition*, 138, 103631. <https://doi.org/10.1016/j.bandc.2019.103631>
- Woodward, T. S., Feredoes, E., Metzak, P. D., Takane, Y., & Manoach, D. S. (2013). Epoch-specific functional networks involved in working memory. *NeuroImage*, 65, 529–539. <https://doi.org/10.1016/j.neuroimage.2012.09.070>
- Woodward, T. S., Leong, K., Sanford, N., Tipper, C. M., & Lavigne, K. M. (2016). Altered balance of functional brain networks in Schizophrenia. *Psychiatry Research: Neuroimaging*, 248, 94–104. <https://doi.org/10.1016/j.psychres.2016.01.003>
- Woodward, T. S., Ruff, C. C., & Ngan, E. T. C. (2006). Short- and long-term changes in anterior cingulate activation during resolution of task-set competition. *Brain Research*, 1068(1), 161–169. <https://doi.org/10.1016/j.brainres.2005.10.094>
- Woodward, T. S., Tipper, C. M., Leung, A. L., Lavigne, K. M., Sanford, N., & Metzak, P. D. (2015). Reduced functional connectivity during controlled semantic integration in schizophrenia: A multivariate approach: Reduced Functional Connectivity. *Human Brain Mapping*, 36(8), 2948–2964. <https://doi.org/10.1002/hbm.22820>
- Zeng, E., Shahki, J., Woodward, T. S. (2024). The Pattern-based Anatomy and Cognitive Mode Associated with the Language Network in fMRI. PsyArXiv. May 28. osf.io/preprints/psyarxiv/c83d7. DOI:10.31234/osf.io/c83d7.